Distinction in the Immunoreactivities of Two Calcium-Binding Proteins and Neuronal Birthdates in the First and Higher-Order Somatosensory Thalamic Nuclei of Mice: Evolutionary Implications

Jiang-Yan Zhang,[1] Yu-Tao Lin,[1] Yuan-Yuan Gao,[1] Chao-Xi,[1] Xue-Bo Zhang,[2] Xin-Wen Zhang,[2]* and Shao-Ju Zeng[1]*

[1]Beijing Key Laboratory of Gene Resource and Molecular Development, Beijing Normal University, PR China
[2]College of Life Sciences, Hainan Normal University, Haikou, PR China

Comparative embryonic studies are the most effective way to discern phylogenetic changes. To gain insight into the constitution and evolution of mammalian somatosensory thalamic nuclei, we first studied how calbindin (CB) and parvalbumin (PV) immunoreactivities appear during embryonic development in the first-order relaying somatosensory nuclei, i.e., the ventral posteromedial (VPM) and posterolateral (VPL) nuclei, and their neighboring higher-order modulatory regions, including the ventromedial or ventrolateral nucleus, posterior, and the reticular nucleus. The results indicated that cell bodies that were immunoreactive for CB were found earlier (embryonic day 12 [E12]) in the dorsal thalamus than were cells positive for PV (E14), and the adult somatosensory thalamus was characterized by complementary CB and PV distributions with PV dominance in the first-order relaying nuclei and CB dominance in the higher-order regions. We then labeled proliferating cells with [^{3}H]-thymidine from E11 to 19 and found that the onset of neurogenesis began later (E12) in the first-order relaying nuclei than in the higher-order regions (E11). Using double-labeling with [^{3}H]-thymidine autoradiography and CB or PV immunohistochemistry, we found that CB neurons were born earlier (E11–12) than PV neurons (E12–13) in the studied areas. Thus, similar to auditory nuclei, the first and the higher-order somatosensory nuclei exhibited significant distinctions in CB/PV immunohistochemistry and birthdates during embryonic development. These data, combined with the results of a cladistic analysis of the thalamic somatosensory nuclei, are discussed from an evolutionary perspective of sensory nuclei. J. Comp. Neurol. 523:2738–2751, 2015.

INDEXING TERMS: somatosensory nuclei; core-to-matrix organization; neurogenesis; brain evolution; AB_2174013; AB_10000340

Inextricably complex brain structures are more conserved among vertebrates than previously believed with respect to their anatomical positions, cytoarchitectures, neural connectivities, immunochemistries, and expression of regulatory homeobox genes (Striedter, 1997; Puelles et al., 2000). However, as brains do not fossilize it remains a challenging task to reconstruct the evolutionary process of brain organization. To resolve this issue, additional brain studies and phylogenetic comparisons are needed.

Based on their immunoreactive properties and neural connections, thalamic relay regions for auditory (the medial geniculate body), somatosensory (the ventral posterior complex and its environs), and visual (the dorsal lateral geniculate nucleus) inputs consist of a core region and adjacent diffuse areas (Jones, 1998; Durand et al., 1992; Zeng et al., 2004). The core region

The first two authors contributed equally to this work.

Grant sponsor: National Natural Science Foundation of China; Grant numbers: 30970951 and 31172082 (to S.J.Z), 31160205, 31360517, 31360243 (to X.B.Z.).

Correspondence to: S.J. Zeng, Beijing Key Laboratory of Gene Resource and Molecular Development, Beijing Normal University, Beijing, 100875, PR China. E-mail: sjzeng@bnu.edu.cn or X.W. Zhang, College of Life Sciences, Hainan Normal University, Haikou, 571158, PR China. E-mail: zhangxw2488@sina.com

Received January 9, 2015; Revised May 14, 2015;
Accepted May 14, 2015.
DOI 10.1002/cne.23813
Published online July 16, 2015 in Wiley Online Library (wileyonlinelibrary.com)

is dominantly composed of PV cells and is compactly cytoarchitecturally organized. This region is closely linked to the peripheral sense organs, receives afferents from subcortical inputs that have readily identifiable physiological properties, and are topographically precise, and project in an area-specific manner to the middle layers of the cerebral cortex in a highly ordered fashion. The core region and its neural pathways are involved in sensory relay or perception (Koralek et al., 1988; Durand et al., 1992; Jones, 2001; Zeng et al., 2004). In contrast, the surrounding diffuse areas are dominantly composed of CB cells and are diffusely organized with relatively small cells (Brauth and Reiner, 1991; Puelles et al., 1994; Belekhova et al., 2002; Peruzzi and Dut, 2004). These areas are less closely linked to the periphery, receive afferents from subcortical inputs that lack the topographic order and physiological precision, and project to superficial layers of the cerebral cortex over relatively wide areas and to subcortical areas that are involved in sensory-mediated physiological responses such as auditory-associated defensive, aggressive, and emotional behaviors (Huffman and Henson, 1990; Durand et al., 1992; Pritz and Stritzel, 1992; Chen and Zuo, 1994).

Neurons in the core region respond rapidly and vigorously to stimuli in a topographical manner (Durand et al., 1992; Wild et al., 1993; Jones, 1998; Ahissar and Zacksenhouse, 2001). In contrast, neurons in the diffuse areas respond relatively slowly and are not tonotopically organized (Diamond et al., 1992; Friedberg et al., 1999). Markers of metabolic activity, such as cytochrome oxidase (CO) and 2-deoxyglucose (2-DG), are primarily restricted to the core regions of auditory nuclei (Paton et al., 1982; Dezso et al., 1993; Hevner et al., 1995). Our recent studies have shown that the germinal sites for the progenitor cells of the auditory core and diffuse areas are located in different regions of the ventricular zone, and the lengths of the cell cycle and S-phase in the diffuse areas are both longer than those in the core region, which results in greater mitotic activity in the core region compared to that in the shell areas (Xi et al., 2011).

Interestingly, although a clear core-to-shell organization is evident in the auditory nuclei of amniotes, this organization is present in amphibian mesencephalic auditory areas and is not present in amphibian diencephalic auditory areas or the mesencephalic and diencephalic auditory areas of teleost fishes (Feng and Lin, 1991; Crespo et al., 1999; Zeng et al., 2007a). Nevertheless, these areas that lack clear core-to-shell auditory organization in amphibians and teleost fishes exhibit features that are similar to those of the shell auditory areas of amniotes, including diffuse neural connectivity and a lack of topographic order and physiological precision (Cuadrado, 1987; Schellart et al., 1987; McCormick, 1999, 2001; Bass et al., 2000). These cladistic analyses suggest that the shell region might be a more phylogenetically ancient configuration than the core region across the evolutionary course of vertebrates.

Additionally, the generation of cells in the core auditory regions of amniotes is significantly delayed in the ventricle zone relative to the cells in the diffuse regions (Zeng et al., 2007b, 2008a,b, 2009), and positive CB staining occurs earlier than PV immunoreactivity during embryonic development (Xi et al., 2011). In light of the concept of Von Baerian recapitulation, early animal embryos within a taxon resemble each other, and the degree of resemblance decreases as development proceeds (Gould, 1977; Butler, 1994; Northcutt, 1990, 2001). Accordingly, the shell region that is generated earlier in embryonic development might be more phylogenetically ancient than the core region, which is consistent with the above conclusion obtained from cladistic analysis.

Based on the neural connections and physiological activities, somatosensory thalamic nuclei, like auditory nuclei, have been shown to consist of two parts, the first-order thalamic relaying nuclei and the higher-order modulatory nuclei (Jones, 1998, 2001). The former include the ventral posteromedial (VPM) and posterolateral (VPL) nuclei, and they receive somatosensory inputs from the dorsal column and external cuneate nuclei or from the trigeminal nucleus, which are topographically precise and have readily identifiable electrophysiological properties (Williams et al., 1994; Sherman et al., 1996; Herbert et al., 2003; Viaene et al., 2011). These nuclei send projections in highly ordered fashion to layer IV of the primary somatosensory cortex, and are identified as the transmitter of receptive field properties (Sherman and Guillery, 1998). The first-order thalamic relaying nuclei are a core of cells distinguished by immunoreactivity for PV (Jones, 1998). In contrast, the higher-order modulatory nuclei, including the ventromedial (VM) thalamic nucleus, the posterior (PO), and the ventrolateral (VL) thalamic nuclei, receive information about somatosensory stimuli and body movements, widespread cutaneous nociceptive inputs (Lenz et al., 1994; Monconduit et al., 1999, 2003; Desbois and Villanueva, 2001), or somatosensory stimuli from the interpolar part of the extralemniscal inputs of the spinal trigeminal nucleus (Spreafico et al., 1987; Veinante et al., 2000; Landisman et al., 2007). These somatosensory inputs commonly lack easily definable receptive fields and show less precise stimulus-response coupling (Jones, 1998, 2001). The higher-order modulatory areas send projections to the entire layer I of the dorsolateral

neocortex (Villanueva et al., 1996, 1998; Stepniewska et al., 2003; Sherman, 2007). Thus, based on the neural connections or activities and chemical identities, the first- and higher-order thalamic somatosensory nuclei largely correspond to the "core" and the "shell" auditory nuclei.

Although there are some reports about neurogenesis in the mammalian brain (Angevine, 1970; McAllister et al., 1977; Altman and Bayer, 1979, 1988, 1989), it remains unclear whether a clear distinction exists in embryonic genesis between the first- and higher-order thalamic somatosensory nuclei. Additionally, how CB and PV immunohistochemistry appear gradually during the development of thalamic somatosensory nuclei remains unknown. Because early comparative embryogenesis might reflect the organization and evolutionary aspects of brain areas, the above issue is worth studying.

In the present study, we first examined how CB and PV immunoreactivities appear and change during embryonic development in the core and diffuse thalamic somatosensory regions. We then labeled proliferating neuronal precursors in embryonic (E) day 11 to 19 mouse embryos with [^{3}H]-thymidine. At postnatal day 30, we quantified the [^{3}H]-thymidine-labeled cells in the VPM/VPL and the higher-order thalamic modulatory regions, including PO, VM, VL, and reticular nucleus (Rt). We also employed double-labeling with [^{3}H]-thymidine autoradiography and CB or PV immunohistochemistry to determine the birthdates of the CB and PV cells in the thalamic somatosensory regions.

MATERIALS AND METHODS

Animals and immunohistochemistry for CB and PV

Adult CD1 mice (*Mus musculus*) aged 7–9 weeks and weighing 20–30 g were housed with ad libitum access to both food and water on a light:dark cycle (12/12-hour on/off) in a temperature-controlled (23°C) environment. Female mice were coupled with males between 4 PM and 6 PM. E1 was defined as the day of plug detection. The embryos from the following stages of E12 to E19 were studied.

Abbreviations

3V	Third ventricle
CB	Calbindin
DLG	Dorsal lateral geniculate body
LD	Laterodorsal thalamic nucleus
LV	Lateral ventricle
PO	Posterior thalamic nucleus
PV	Parvalbumin
Rt	Reticular nucleus
VL	Ventrolateral thalamic nucleus
VM	Ventromedial thalamic nucleus
VPL	Ventral posterolateral thalamic nucleus
VPM	Ventral posteromedial thalamic nucleus

We also used 30-day-old mice with well-developed brains to study CB or PV immunohistochemistry in the thalamic somatosensory regions. The animals were deeply anesthetized with sodium pentobarbital and perfused through the heart with phosphate-buffered saline (PBS) and 4% paraformaldehyde in 0.1 M sodium phosphate buffer (PB) at a pH of 7.4. The brains were removed and postfixed in the same fixative for 6 hours. Mice or chicken embryo heads or dissected brains at scheduled stages were also fixed in the same fixative for 24 (for small brains) or 48 (for large brains) hours. The brains were cryoprotected in 30% sucrose overnight. The brains were then embedded in gelatin-sucrose and sectioned at 10 μm. Every eighth section was mounted onto a gelatin-coated slide. These sections were subjected to Nissl staining or CB and PV immunohistochemistry. All experiments were performed in accordance with the guidelines for animal care provided by the Beijing Animal Administration Committee.

For PV and CB immunohistochemistry, a set of sections was pretreated for 15 minutes with 3% hydrogen peroxide in 80% methanol, blocked for 2 hours (3% normal goat serum / 0.5% Triton X-100 in PBS), and incubated overnight at 4°C with primary antiserum against CB (1:2,000; Swant, Bellinzona, Switzerland) and PV (1:1,500; Chemicon, Temecula, CA). After washing with PBS, the sections were incubated in a biotinylated goat antirabbit IgG antibody (for CB, 1:400, BA-1000, Vector Laboratories, Burlingame, CA) or in a biotinylated horse antimouse IgG antibody (for PV, 1:500, ZB-2020, Zymed, San Francisco, CA) for 2 hours at room temperature (RT). The sections were then washed and reacted with an avidin-biotin-peroxidase complex (1:150, Elite ABC kit, Vector) for 2 hours at RT. The sections were subsequently incubated in 3,3′-diaminobenzidine (DAB; Sigma, St. Louis, MO) for 30 minutes at RT.

[^{3}H]-thymidine autoradiography and double-labeling for PV or CB immunohistochemistry and [^{3}H]-thymidine autoradiography

Pregnant mice were injected subcutaneously with a single dose of [^{3}H]-thymidine (specific activity, 6.7 Ci/mM; Amersham Pharmacia Biotech, UK; 2.5 μCi/g body weight) on each day from E11 to E19. The injections were performed at 9:00 AM. The litters were weaned at 3 weeks after birth and grew to the age of 30 days.

The mice were deeply anesthetized and the brains were perfused, postfixed, and cut on a freezing microtome (Leica, Germany) as described above. A total of six sets of sections were obtained from each brain and processed for either single [^{3}H]-thymidine autoradiography, double-labeling for PV or CB immunohistochemistry,

TABLE 1.
Primary Antibodies Used

Antigen	Description of immunogen	Source, host species, Cat. #, RRID	Concentration used
Parvalbumin	The antibody is directed against an epitope at the first Ca^{2+}-binding site and specifically stains the Ca^{2+} -bound form of parvalbumin. Frog muscle PV antigen	Merck Millipore, mouse monoclonal, # MAB1572, RRID: AB_2174013 PubMed ID: 23254904	1:1,500 dilution
Calbindin D-28K	Recombinant rat calbindin corresponding to rat calbindin D-28K.	Swant (Bellinzona, Switzerland), rabbit polyclonal, #CB-38a RRID: AB_10000340 PubMed ID: 21800302	1:2,000 dilution

and [^{3}H]-thymidine autoradiography immunohistochemistry or Nissl staining. For single [^{3}H]-thymidine autoradiography, a set of sections was processed with an alcohol-water series and xylene and dried at 37°C. The sections were then covered with Kodak NTB-2 emulsion, maintained at 4°C for an exposure period of ~4 weeks in light-tight boxes, and then developed in D19 (Kodak, Rochester, NY). To visualize the tissue cytoarchitectures and cellular morphologies, the sections were counterstained with cresyl violet. The detailed autoradiographic procedures have been previously described (Zeng et al., 2007b).

For double-labeling for PV or CB immunohistochemistry and [^{3}H]-thymidine autoradiography, sets of sections were first used for PV or CB immunohistochemistry staining and subsequently processed with [^{3}H]-thymidine autoradiography as described above.

Antibody characterization

Please see Table 1 for a list of all antibodies used. The mouse monoclonal antibody for PV recognized a protein of 12 kDa on western blot of mouse brain lysate. This antibody is directed against a synthetic peptide, an epitope in the first calcium-binding site. This antibody staining showed a single band (12 kDa) on western blot for many species, including fish, frog, chicken, and mouse. Immunostaining is completely eliminated when the antibody is incubated with the immunogen peptide prior to staining. In this study the immunostaining of this antibody showed similar size, shape, and distribution with these reports (Jones and Hendry, 1989; Jones, 1994, 1998; Yang et al., 2008).

The rabbit polyclonal CB D-28k antibody recognized a single band of ~27–28 kDa on immunoblot of brain homogenate of various species including rat, mouse, chicken, and fish. Antiserum CB38 did not stain the brains of CB D-28k knockout mice (manufacturer's technical information). Staining with this antibody in the present study revealed the similar cellular morphology with previous reports on mouse brain (Orduz et al., 2014).

Controls were also carried out by omitting either the primary or the secondary antibody, with all other steps in parallel with the above, to ensure that crossreactivity was not an issue. Omitting either primary or secondary antibody abolished immunostaining.

Images, cell counting, and statistics

Immunolabeled sections were viewed with an Olympus (BH-2) microscope (Olympus, Japan). The images were captured with a digital camera (Spot Enhance 2e, Diagnostic Instruments, Sterling Heights, MI) attached to the microscope. The contrast and brightness were adjusted using Adobe Photoshop (Adobe 8.0, Mountain View, CA).

A cell was regarded as labeled if the autoradiographic grains overlying its nucleus exceeded six times the background level, which was separately determined for each specimen. All of the studied areas were evaluated at a magnification of 400× with the aid of an ocular grid.

To find potential gradients of neurogenesis along the rostral-to-caudal neuraxis in studied thalamic areas, labeled cells were examined in three coronal planes with equal intervals (from the initial appearance of the VL to the end of the VPM, two ends of the whole somatosensory region): the medial plane through which the thalamic somatosensory area was divided in half, the rostromedial and the caudomedial planes through which the thalamic somatosensory area was divided in half from the most rostral to the medial or from the medial to the most caudal, respectively. These planes and the nomenclature for the subdivisions of the thalamic somatosensory areas were consulted the mouse stereotaxic atlas of Bao and Shu (1990), the mouse atlas of Franklin and Paxinos (1997), or the rat atlas of Swanson (1998). Only cells with clear nuclei and relatively large cytoplasm were regarded as neurons and counted.

All of the labeled neurons and the total neurons (labeled and unlabeled) were counted at three chosen levels (rostromedial, medial, and caudomedial) of the entire somatosensory thalamic region. The data are expressed as the percentage of labeled neurons (the number of labeled neurons/the total number of

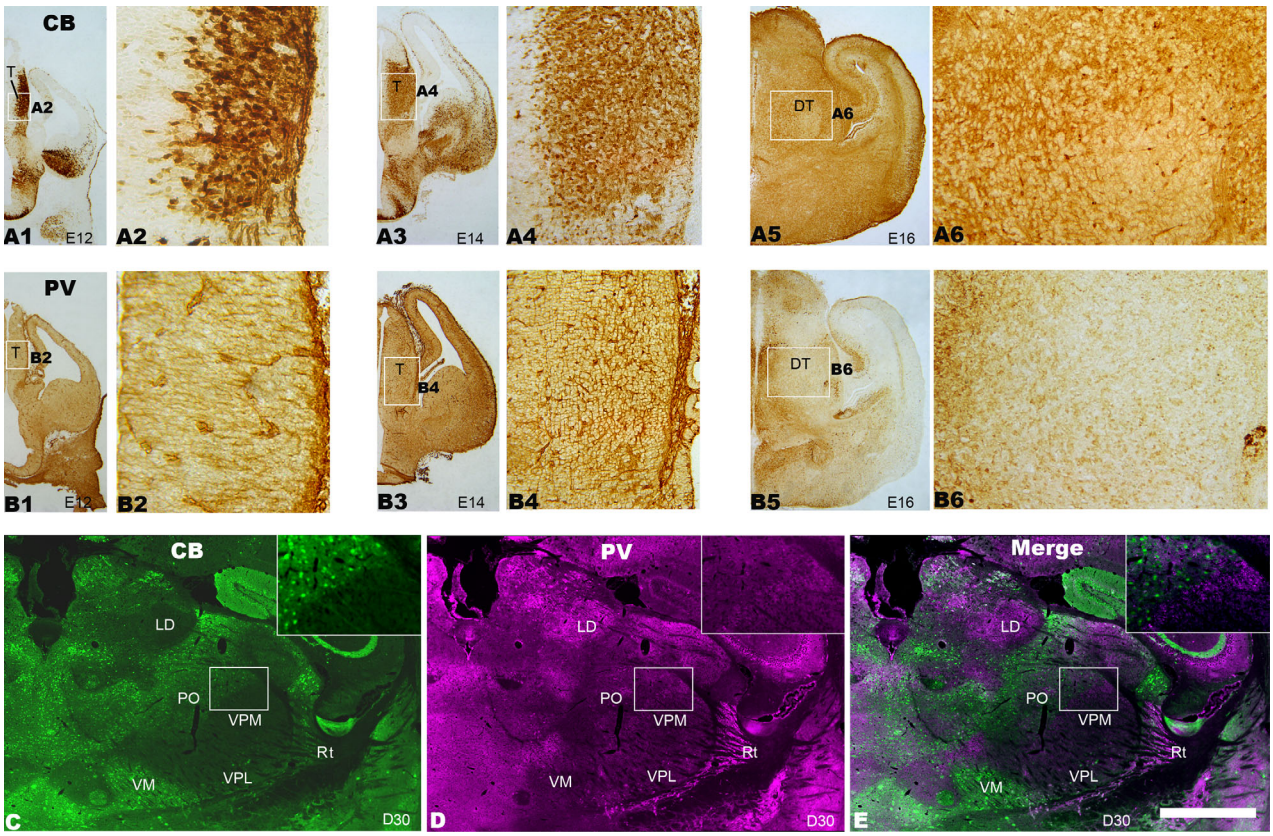

Figure 1. Photomicrographs of coronal sections through the somatosensory thalamus of a mouse showing the distributions of calbindin (CB) and parvalbumin (PV) cells during embryonic development and at the age of 30 days. **A1–A6:** CB distribution at E12 (A1 and A2), E14 (A3 and A4), and E16 (A5 and A6). **B1–B6:** PV distribution at E12 (B1 and B2), E14 (B3 and B4), and E16 (B5 and B6). The boxed areas in A1, A3, A5, B1, B3, and B5 are amplified in A2, A4, A6, B2, B4, and B6, respectively. **C–E:** Double-labeling for CB and PV at the age of 30 days (D30). (C: Single-labeling for CB, D: Single-labeling for PV, E: Merge of C,D). The small boxed areas in C–E are further amplified in the inserts. For abbreviations, see list. Scale bar = 600 μm in E for B1, B3, and B5 (50 μm for A2 and B2, 75 μm for A4 and B4, 100 μm for A6 and B6); 300 μm for C–E (125 μm for the inserts). [Color figure can be viewed in the online issue, which is available at wileyonlinelibrary.com.]

neurons × 100%). Both the left and right hemispheres were analyzed. No significant differences in the percentages of labeled neurons between the two hemispheres were observed, and the data from the two hemispheres were thus combined for each brain level. Coronal sections from 4–5 mice from each injection group were used for the above quantitative measurements. The percentages of labeled neurons were averaged for each brain level within each group studied and are presented as the means ± SEM. All analyses were performed blind using coded specimens.

Analyses of variance (ANOVAs) were used to compare the averages (dependent variables) between the different age groups (independent variables) using SPSS for Windows 11.0 (Chicago, IL). All data subjected to ANOVAs were normally distributed (one-sample Kolmogorov-Smirnov test), and post-hoc comparisons were made with Fisher's protected least significant difference (PLSD) tests. Student's *t*-tests were used to compare the differences in the percentages of labeled neurons between two parts of a studied area and between pairs of different age groups. Significance was set at $P \leq 0.05$.

RESULTS

The present study focused on the thalamic somatosensory relays, the VPM and VPL, and their neighboring regions, PO, VM, VL, and Rt. Along the rostral-to-caudal axis, the VPL and the Rt appeared in all three of the examined coronal brain levels (i.e., rostromedial, medial, and caudomedial), while the VPM, VM, and PO were present in the medial and caudomedial levels, and the VL appeared only in the rostromedial level (Figs. 1C–E and 2A–I).

CB and PV immunohistochemistry

CB and PV immunostaining were performed at interval from E12 to E19 and at the age of 30 days. At E12,

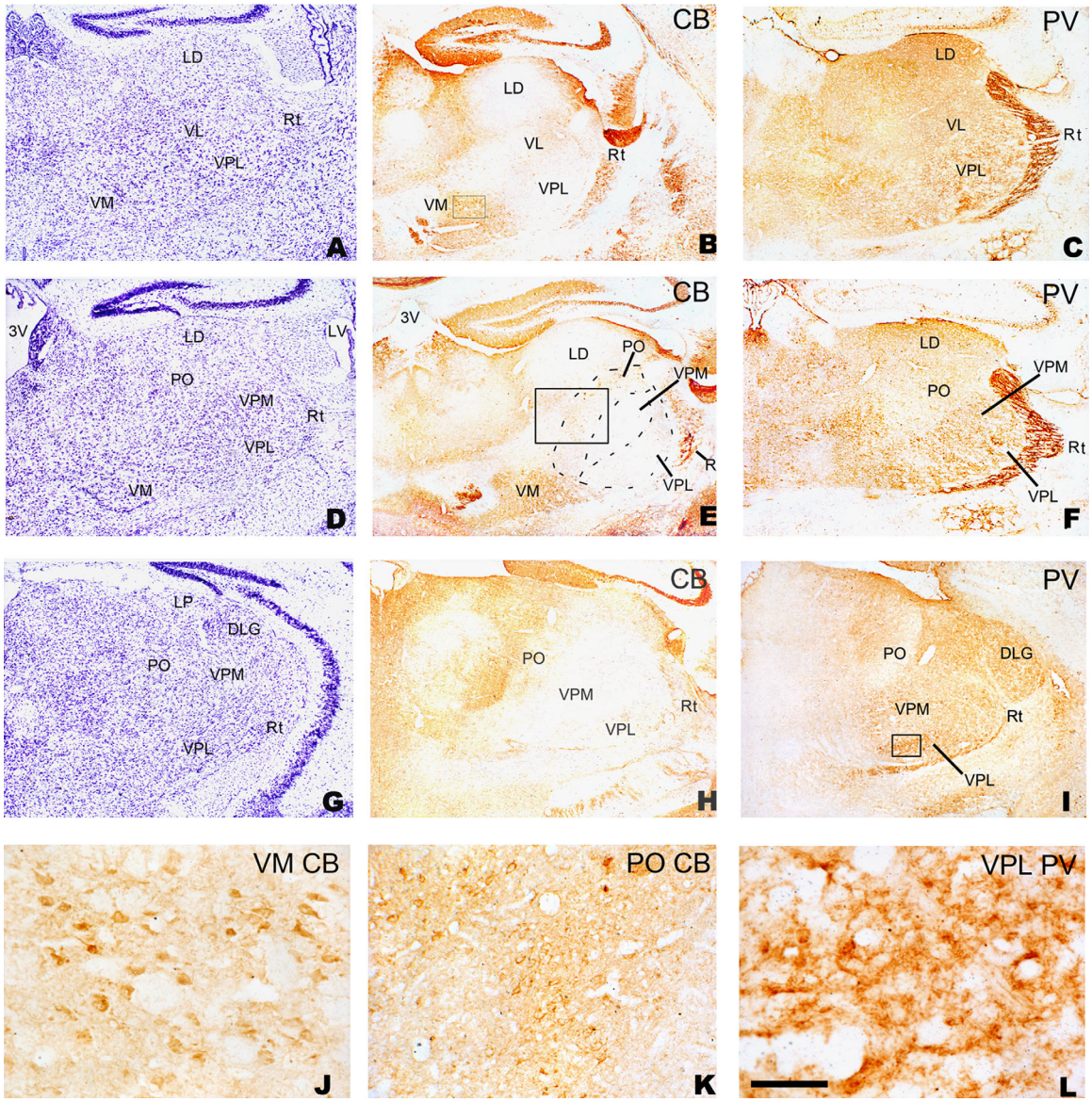

Figure 2. Photomicrographs of coronal sections through the somatosensory thalamus of a mouse showing the principal thalamic relays, the ventral posterolateral thalamic nucleus (VPL), the ventral posteromedial thalamic nucleus (VPM), and their neighboring regions. **A–I:** Coronal sections at the rostromedial (A–C), medial (D–F), and caudomedial (G–I) brain levels of the entire somatosensory region (from the initial appearance of the ventrolateral thalamic nucleus to the end of the VPM rostrocaudally) with Nissl staining (A,D,G), calbindin immunohistochemistry (B,E,H), and parvalbumin immunohistochemistry (C,F,I). **J–L:** Magnified areas of the boxed regions in B,E,I, respectively. For other abbreviations, see list. Scale bar = 300 μm for A–I, 50 μm for J,L, 100 μm for K. [Color figure can be viewed in the online issue, which is available at wileyonlinelibrary.com.]

the cell bodies that were immunoreactive for CB had already appeared along the outer part of the ventricle wall in the dorsal thalamus (Fig. 1A1,A12). At E14, the ventricle wall in the dorsal thalamus became thicker, and more CB-positive cell bodies were observed to be distributed across a larger area of the dorsal thalamus (Fig. 1A3,A4). From E16 onwards, the CB cells were unevenly diffused into the entire dorsal thalamus (Fig. 1A5,A6). At E19, the brain structures in the dorsal thalamus were much like those observed at the age of 30 days in that the CB immunoreactivity was nearly absent from the VPM and VPL (Figs. 1C–E, 2B,E,H), and only a few small CB cells were scarcely distributed in the VPL (Figs. 1C,E, 2H). In contrast, positive staining for CB was observed in the neighboring regions of the VPM and VPL, including the VL (Fig. 2B), VM (Figs. 1C,E, 2B,E,J), PO (Figs. 1C,E, 2E,H,K), and Rt (Figs. 1C,E, 2B,E,H, 5A,C).

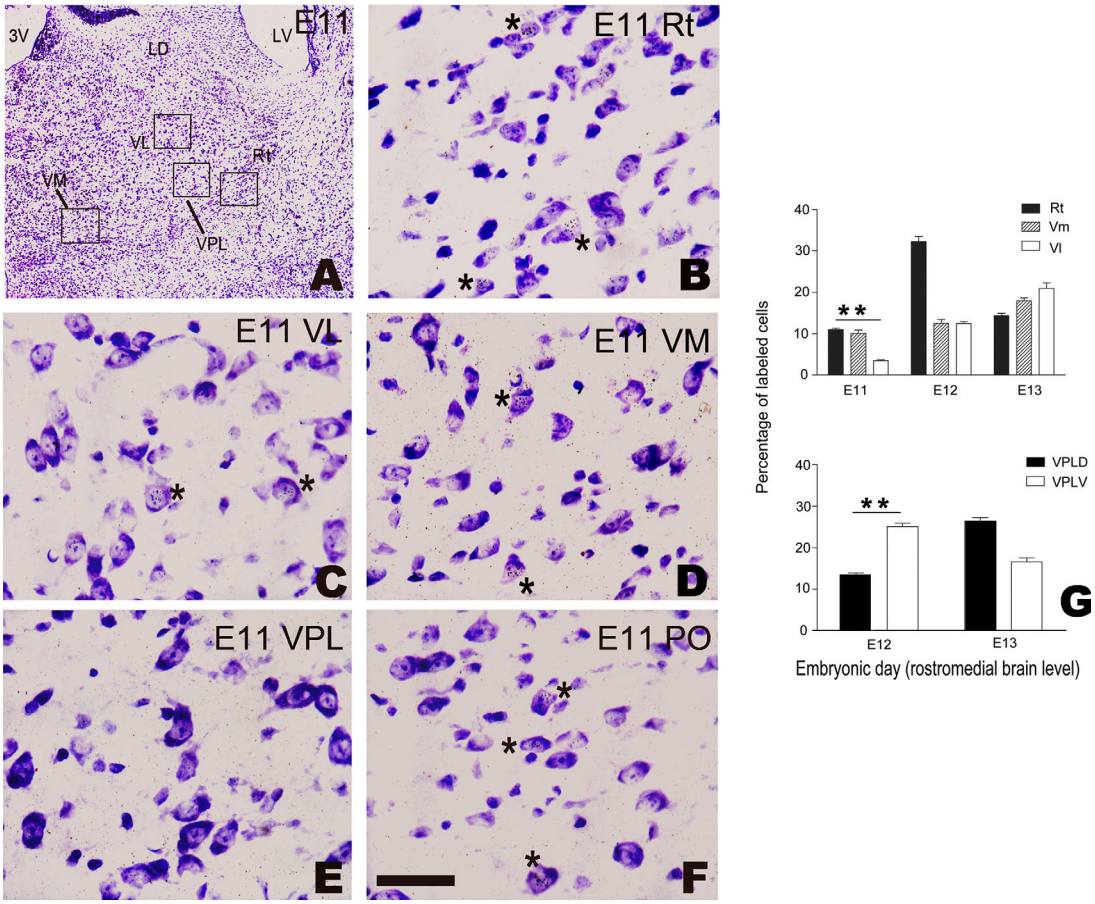

Figure 3. [^{3}H]-thymidine labeling in the somatosensory thalamus of a mouse. **A:** A section counterstained with cresyl violet showing the locations of B–E. **B–F:** [^{3}H]-thymidine labeling in the reticular nucleus (Rt) (B), ventrolateral thalamic nucleus (VL) (C), ventromedial thalamic nucleus (VM) (D), ventral posterolateral thalamic nucleus (VPL) (E), and posterior thalamic nucleus (PO) (F) following [^{3}H]-thymidine injection at embryonic day 11 (E11). Some [^{3}H]-thymidine-labeled neurons are marked by stars. Note that no [^{3}H]-thymidine-labeled neurons were present in the VPL. **G:** The percentages of [^{3}H]-thymidine-labeled cells at the rostromedial brain level. **Significant differences between the studied age groups. For other abbreviations, see list. Scale bar = 300 μm for A and 50 μm for the other panels. [Color figure can be viewed in the online issue, which is available at wileyonlinelibrary.com.]

At E12, cell bodies that were immunoreactive for PV were not observed in the ventricle wall of the dorsal thalamus. However, immunoreactive fibers were clearly observed to extend within the ventricle wall of the dorsal thalamus (Fig. 1B1,B2). At E14, cell bodies that were immunoreactive for PV appeared in the ventricle wall of the dorsal thalamus (Fig. 1B3,B4). From E16 onwards, the PV cells were unevenly distributed across the entire dorsal thalamus (Fig. 1B5,B6). At E19, the distribution of PV cells was similar to that at the age of 30 days. PV immunohistochemistry was evident in the VPM and VPL (Figs. 1D,E, 2C,F,I,L). Some PV-labeled cells and tiny fibers were detected in the VPM and VPL (Figs. 2L, 5I). Strong staining for PV (including labeled cells and fibers) occurred in the Rt (Figs. 1D,E, 5F,G). Our double-labeling for CB and PV indicated that no cells that were double-labeled for CB and PV were observed in the studied sensory thalamic areas (Fig. 1C–E).

Single [^{3}H]-thymidine autoradiography

[^{3}H]-thymidine-labeling was examined in the VPM and VPL and the neighboring regions (i.e., PO, VM, VL, and Rt) at three rostral-to-caudal brain levels (i.e., rostromedial, medial, and caudomedial). Because the VPM and VPL are relatively large areas, they were further divided into dorsal-ventral halves to detect any potential gradient of neurogenesis. Nissl staining and CB/PV immunohistochemistry were both employed to accurately identify the subdivisions of the thalamic somatosensory areas (Fig. 2).

The earliest [^{3}H]-thymidine-labeled cells appeared in the E11 age group, and [^{3}H]-thymidine-labeled cells disappeared after E14. In the E11 age group, labeled cells

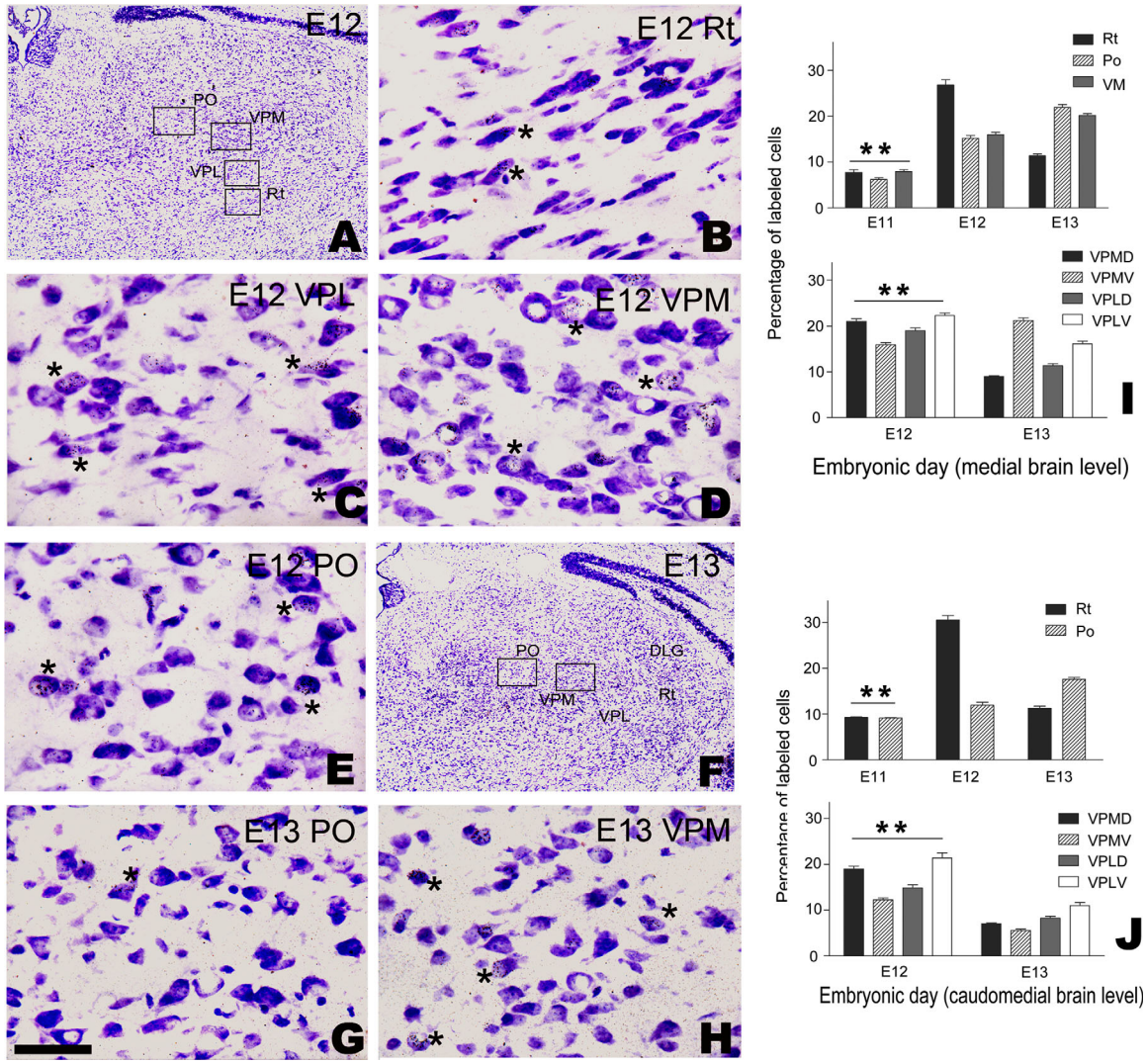

Figure 4. [^{3}H]-thymidine labeling in the somatosensory thalamus of a mouse. **A:** A section counterstained with cresyl violet showing the locations of B–E. **B–E:** [^{3}H]-thymidine labeling in the reticular nucleus (Rt) (B), ventral posterolateral thalamic nucleus (VPL) (C), ventral posteromedial thalamic nucleus (VPM) (D), and posterior thalamic nucleus (PO) (E) following [^{3}H]-thymidine injection at embryonic day 12 (E12). **F:** A section counterstained with cresyl violet showing the locations of G,H. **G,H:** [^{3}H]-thymidine labeling in the PO and VPM following [^{3}H]-thymidine injection at E13. Some [^{3}H]-thymidine-labeled neurons are marked by stars. **I,J:** Percentages of [^{3}H]-thymidine-labeled cells at the rostromedial (I) and caudomedial (J) coronal brain levels. **Significant differences between the studied age groups ($P < 0.001$). For other abbreviations, see list. Scale bar = 300 μm for A and F and 50 μm for the other panels. [Color figure can be viewed in the online issue, which is available at wileyonlinelibrary.com.]

were present in all of the studied regions neighboring the VPM and VPL, including the Rt (Fig. 4B), VL (Fig. 4C), VM (Fig. 4D), and PO (Fig. 4F). However, there were very few labeled cells in the VPM and VPL themselves (Fig. 4E). [^{3}H]-thymidine-labeled cells were evident in the VPM and VPL in the E12 age group (Fig. 5C,D) and reached a peak in the E13 age group at the medial and caudomedial brain levels (Fig. 5H,J). There were significant differences between the dorsal and ventral VPL at E12 ($t = -5.651$, $P < 0.001$), and no significant differences were detected at E13 ($t = 0.406$, $P = 0.724$). A two-way ANOVA indicated that there were significant differences between the neurogenesis gradients in the three examined coronal brain levels (i.e., rostromedial, medial, and caudomedial) in the dorsal VPL (VPLD) ($F = 113.25$, $P < 0.001$), the ventral VPL (VPLV) ($F = 30.346$, $P < 0.001$), the VL ($F = 30.575$, $P < 0.001$), and the Rt ($F = 46.127$, $P < 0.001$) (Figs. 3G, 4I,J). There were significant differences between the dorsal and ventral VPM at E12 ($t = 4.468$, $P = 0.001$), and no significant differences were detected at E13 ($t = -1.83$, $P = 0.08$). The neurogenesis gradients also exhibited

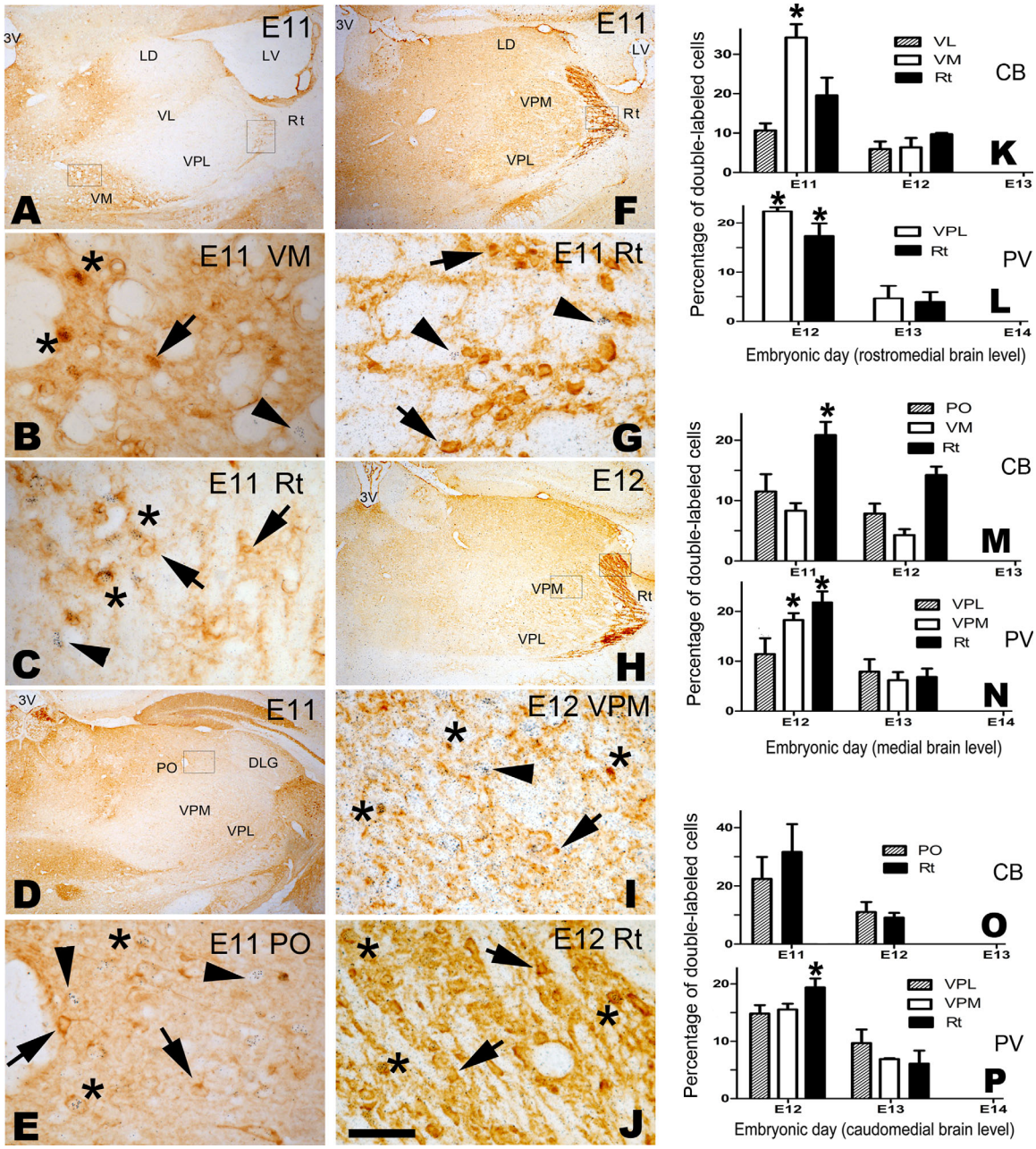

Figure 5. [^{3}H]-thymidine autoradiography combined with immunohistochemistry for calbindin (CB) and parvalbumin (PV). **A–E:** Cells labeled for CB and [^{3}H]-thymidine in the ventromedial thalamic nucleus (VM) (B), reticular nucleus (Rt) (C), and posterior thalamic nucleus (PO) (E) following [^{3}H]-thymidine injection at E11. The approximate locations of B,C,E are shown in the boxed areas in A and D. C is the boxed area of Rt in A rotated clockwise by 90°. **F,G:** Cells labeled for PV and [^{3}H]-thymidine in Rt following [^{3}H]-thymidine injection at E11. G is approximately located in the boxed area in F. There were no cells doubled-labeled for PV and [^{3}H]-thymidine in G. **H–J:** Cells labeled for PV and [^{3}H]-thymidine in the ventral posteromedial thalamic nucleus (VPM) (I) and Rt (J) following [^{3}H]-thymidine injection at E12. The locations of I and J are shown in the boxed areas in H. Some cells doubled-labeled for CB/PV and [^{3}H]-thymidine are marked by stars. Some cells that were only labeled by CB/PV or [^{3}H]-thymidine are indicated by arrows and arrowheads, respectively. **K–P:** Percentages of cells doubled-labeled for [^{3}H]-thymidine and CB (K,M,O) or PV (L,N,P) at the rostromedial (K,L), medial (M,N) and caudomedial (O,P) coronal brain levels. *Significant differences between the marked group and its corresponding next age group ($P < 0.05$). For other abbreviations, see list. Scale bar = 300 μm for A,D,F,H,L and 50 μm for the other panels. [Color figure can be viewed in the online issue, which is available at wileyonlinelibrary.com.]

significant differences between the medial and caudomedial brain levels in the dorsal VPM (VPMD) ($F = 1125.045$, $P < 0.001$), the ventral VPM (VPMV) ($F = 1116.38$, $P < 0.001$), and the PO ($F = 1123.656$, $P < 0.001$), and between the rostromedial and medial brain levels in the VM ($F = 10.546$, $P < 0.001$) (Figs. 3G, 4I,J).

Double-labeling with [^{3}H]-thymidine autoradiography and immunohistochemistry for CB or PV

To determine the birthdates of the CB and PV cells in the thalamic somatosensory areas, we examined the numbers of cells from E11 to E19 that were double-labeled for [^{3}H]-thymidine autoradiography and CB at the rostromedial brain level (VL, VM, and Rt), the medial brain level (PO, VM, and Rt), and the caudomedial brain level (PO and Rt) in which the CB cells were distributed, and we also examined the numbers of cells that were double-labeled for [^{3}H]-thymidine autoradiography and PV immunohistochemistry at the rostromedial (VPL and Rt), medial, and caudomedial brain levels (VPL and VPM) in which the PV cells were located. As shown in Figure 5A–E, some [^{3}H]-thymidine-labeled cells also stained positively for CB. However, no [^{3}H]-thymidine-labeled cells positive for PV were found in the studied areas in the same age group (E11) (Fig. 5F,G). The cells that were positively labeled for [^{3}H]-thymidine and PV were observed in the VPM, VPL (Fig. 5H,I) and Rt (Fig. 5H,J) in the E12 and E13 age groups.

CB and [^{3}H]-thymidine double-labeled cells were thus observed earlier (in E11 and E12) than were cells that were double-labeled for PV and [^{3}H]-thymidine (in E12 and E13) in the above-studied areas (Fig. 5K–P). Additionally, the percentages of the cells that were double-labeled for CB and [^{3}H]-thymidine were significantly higher in the E11 age group than in the E12 age group in the VM (at the rostromedial level: $t = 6.768$, $P = 0.003$, Fig. 5M) and PO (at the medial level: $t = 4.725$, $P = 0.01$, Fig. 5M). The percentages PV and [^{3}H]-thymidine double-labeled cells were significantly higher in the E12 age group than in the E13 age group in the VPL (at the rostromedial level: $t = 7.671$, $P = 0.001$, Fig. 5L), VPM (at the medial level: $t = 5.760$, $P = 0.001$, Fig. 5N; at the caudomedial level: $t = 8.453$, $P = 0.000$, Fig. 5P), and Rt (at the rostromedial level: $t = 3.389$, $P = 0.032$, Fig. 5L; at the medial level: $t = 4.675$, $P = 0.001$, Fig. 5N; at the caudomedial level: $t = 4.587$, $P = 0.001$, Fig. 5P).

DISCUSSION

Comparison with previous studies and core-to-matrix organization in somatosensory nuclei of mammals

The present study first examined the dynamic changes in CB and PV immunoreactivity in the dorsal thalamus (in which the somatosensory thalamus is located), and the results indicated that cell bodies that were immunoreactive for CB were already present at E12 in the dorsal thalamus, whereas cell bodies that were positive for PV appeared later at E14. Our results further indicated that the adult somatosensory thalamus is characterized by a general, complementary distribution of CB and PV neurons across the first-order thalamic relays (i.e., the VPM and VPL) to the higher-order modulatory regions (i.e., the PO, VM, and VL). Our results are essentially in agreement with previous studies on the distributions of CB and PV in the adult mammalian thalamus (Jones and Hendry, 1989; Rausell and Jones, 1991; Rausell et al., 1992; Herron et al., 1997; Münkle et al., 2000) with the exception of the following difference. Although some previous reports have shown that CB neurons are primarily located in the neighboring regions of the VPM and VPL, some CB cells have also been observed to occur in the VPL or VPM in the primate (Rausell and Jones, 1991; Rausell et al., 1992). In the present study, a few CB cells were observed in the VPM and VPL. According to previous reports, the CB-positive cells in the "matrix" domains of the VPM and VPL are small, cytochrome-oxidase weak (Jones, 1998). They are innervated by spinothalamic and caudal trigeminal (nonlemniscal) inputs and project to layer I of a wide area of sensory cortex (Jones, 1998, 2001). Thus, CB cells in VPM and VPL should be ascribed to the higher-order modulatory relaying cells (Khachunts and Belekhova, 1986; Rausell et al., 1992; Herron et al., 1997).

Our above findings show that, like primate species, mice also possess a matrix of diffusely and superficially projecting, smaller thalamocortical cells upon which a core of more specifically projecting relay cells is imposed (Jones, 1998, 2001). It has been shown that thalamic neurons receive not only massive sensory-related cortical inputs, but they also receive significant amounts of motor-related information through collaterals of neurons in cortical layer 6 (Sherman and Guillery, 1998; Alitto and Usrey, 2003; Lam and Sherman, 2010). In addition, neurons in the higher-order nuclei also receive innervations from cortical layer 5 (Sherman and Guillery, 1998; Miyata, 2007). These corticothalamic neurons exert both an excitatory and an inhibitory influence on many of the activity patterns and sensory response properties of thalamic neurons (Sherman, 2012; Ahissar and Oram, 2015; Yu et al., 2015). In turn, the higher-order nuclei send projections to many wide cortical regions as well as the first-order nuclei, whereas the first-order nuclei send projections to cortical layer 4 (Groenewegen and Berendse, 1994; Macchi and Bentivoglio, 1999; Guillery and Sherman, 2002). These closed neural loops play roles in corticothalamic or corticocortical communication and in modulating the transfer of information in the thalamus (Sherman and Guillery, 2002; Ahissar and Oram, 2015). In addition, neurons in the modulatory matrix, recruited by

corticothalamic connections, can affect somatosensory activities across thalamic nuclei and cortical areas (Sherman and Guillery, 2002; Sherman, 2012; Ahissar and Oram, 2015; Yu et al., 2015).

Compared to the distribution of CB cells in primates, the present study indicated that many fewer CB cells appeared in the "matrix" of the VPM and VPL in mice. It needs to be mentioned that nearly no CB cells are found in the core auditory nuclei in the mesencephalon or diencephalon of chick (Zeng et al., 2008b), but some are located in the mouse (Zeng et al., 2009). Based on the above analysis of the actions of the higher-order modulatory cells (including CB cells in the matrix of the VPM and VPL), the lack or the large reduction in the number of CB cells in the primary (or the first-order) thalamic relay nuclei might suggest a weak modulation to the transferring thalamocortical information or to the corticocortical communication in mice and birds in comparison with that in primate species. These data reveal that the organizational pattern of thalamic nuclei consisting of phylogenetically ancient (CB cells in the modulatory matrix) and new cells (PV cells in the core or the first-order nuclei) vary across different groups of animals (mammals vs. birds or primates vs. nonprimates in mammals), which might reflect a different evolutionary process of animals. However, this issue is far more complex and needs further study in the future.

Our single [^{3}H]-thymidine autoradiographic data indicated that the onset of neurogenesis began earlier (E11) in the neighboring regions (PO, VM, VL, and Rt) of the VPM and VPL than in the VPM and VPL (E12). Our double-labeling with [^{3}H]-thymidine autoradiography and immunohistochemistry for CB or PV further indicated that, although CB and PV neurons were both present in the Rt, only CB neurons were generated at E11, and PV neurons were produced after E11. These data indicate that the CB neurons were born earlier than the PV neurons in the somatosensory thalamus, which is consistent with the result that CB-stained cells are already present at E12, but PV-stained cells appear later, at E14 in the dorsal thalamus.

It is not clear why a series of studies that sought to determine the birth dates of neurons in the thalami of rats failed to report any differences in neurogenesis between the somatosensory thalamic nuclei (Altman and Bayer, 1979, 1988, 1989), but this failure might have been due to the adoption of different labeling methods. In the present study, only a single dose of [^{3}H]-thymidine ("pulse labeling") was injected into the mice. In contrast, "cumulative labeling" was applied in the previous reports, in which two successive daily doses of [^{3}H]-thymidine were injected into the rats (Altman and Bayer, 1979, 1988, 1989). Pulse labeling might be necessary to distinguish between brain regions with very close birth dates, such as the principal somatosensory thalamic nuclei and their adjacent areas. A nucleus might have different lasting periods of neurogenesis by using the above two labeling methods, and "cumulative labeling" would have a relatively longer period than "pulse labeling." Indeed, our study showed that neuronal generation ended after E13.5, but the previous report placed the end of neuronal generation after E14.5 (Altman and Bayer, 1988). However, despite the use of different labeling methods, rostrocaudal and ventrodorsal gradients of neurogenesis were similar to those of previous reports (Angevine, 1970; McAllister et al., 1977; Altman and Bayer, 1979, 1988, 1989) as observed in our study. Additionally, the results of our study accord with those of a previous report that showed that Rt is one of the earliest-generated nuclei among the thalamic areas (Altman and Bayer, 1979). It is necessary to note that the above reports only examined neurogenesis in the thalamus from E13.5 and left earlier periods of neurogenesis in the thalamus unexamined (Angevine, 1970; McAllister et al., 1977). We will next study whether CB and PV cells in the somatosensory thalamic areas are generated in different sites of the ventricular zone, which would result in the differences in the times of embryonic genesis as has been observed in the mesencephalic auditory core and shell regions in the reptile (Xi et al., 2011).

In contrast to the other studied areas adjacent to the VPM and VPL, Rt is not a paralemniscal areas because it does not send any direct projections to the cerebral cortex. However, like paralemniscal areas, Rt receives innervations from the brainstem reticular formation, and it sends projections to the VPL and VPM and their adjacent paralemniscal areas, including the PO, VM, and VL (French et al., 1985; Pare et al., 1988; Cornwall et al., 1990). It has been further shown that Rt is one of the main sources of inhibitory input to the VPL and VPM and their adjacent paralemniscal areas, which suggests that Rt is involved in the regulation of somatosensory activities (French et al., 1985; Guillery and Sherman, 2002; McAlonan and Brown, 2002; Iwona et al., 2003). From the perspective of neural connectivity and embryonic genesis, Rt, along with other areas adjacent to the VPL and VPM (including the PO, VM, and VL), is very similar to the areas adjacent to the core auditory areas in the thalamus such as the MGd and MGm in mice (related to the MGv core region) and the Ov shell in birds (related to the Ov core region), which are all involved in auditory-mediated electrophysiological activities and produced earlier than the core regions (Huffman and Henson, 1990; Pritz and Stritzel, 1992; Durand et al., 1992; Zeng et al., 2004, 2008b, 2009).

Core-to-matrix organization in somatosensory areas of nonmammals

In other terrestrial vertebrates (e.g., amphibians, reptiles, and birds), two ascending somatosensory pathways have been reported: 1) a primary afferent ascending spinal projection through the dorsal funiculus to the dorsal column nucleus (DCN) that gives rise to the medial lemniscal pathway to the thalamus, and 2) a secondary afferent projection to the reticular formation. In amphibians, the DCN is occupied predominantly by PV neurons (and not CB neurons) and is somatotopically arranged with a medial (gracile) compartment innervated by the dorsal root from its lumber and thoracic segments and a lateral (cuneate) compartment innervated by the cervical enlargement (Muñoz et al., 1995). In the pathway to the thalamus (central, posterior, and ventromedial thalamic nuclei), unlike the fibers in the mammalian lemniscal pathway, the fibers originating in the DCN give off large collaterals to various parts of the reticular formation, the granular layer of the cerebellum, the lateral part of the torus semicircularis, and various tegmental nuclei in the mesencephalon (Muñoz et al., 1995). It is a common feature that somatosensory thalamic nuclei, such as the nucleus anterior in fish, the central, posterior, and ventromedial nuclei in amphibians, the nucleus dorsolateralis anterior in reptiles, and the nucleus dorsolateralis anterior thalami (DLA), dorsolateralis anterior thalami, pars medialis (DLM), and nucleus dorsolateralis posterior thalami (DLP) in birds, all receive inputs from a variety of sources that include the spinal cord, brain stem (the DCN and the reticular formation), and the midbrain and project to separate regions of the telencephalon (striatum, the dorsal ventricular ridge, and the medial or dorsal pallium) (Butler, 1994). To date, no reports have demonstrated an area in nonmammals that strictly corresponds to the mammalian VPM and VPL (the first-order thalamic relays). However, based on neural connectivity some of the thalamic areas mentioned above in the other tetrapods are much more similar to the mammalian paralemniscal thalamic areas, such as the posterior nuclear group (see review of Butler, 1994). From the above phylogenetic analysis of the thalamic nuclei, a preliminary conclusion that the mammalian VPL and VPM might be less phylogenetically ancient than their surrounding areas can be drawn. Therefore, similar to the cladistic analyses of the auditory nuclei in vertebrates mentioned above, phylogenetic analyses of the thalamic somatosensory nuclei also support the suggestion of the primitivity of the paralemniscal subpopulations, as revealed in our embryonic data in light of Von Baer's first law of development (Northcutt, 2001).

ACKNOWLEDGMENTS

We thank Dr. Jin-Liu in Experimental Technology Center for Life Sciences, College of Life Sciences, Beijing Normal University, for technological help.

CONFLICT OF INTEREST

The authors have no known or potential conflicts of interest to declare with respect to the publication of this work.

ROLE OF AUTHORS

All authors had full access to all the data in the study and take responsibility for the integrity of the data and the accuracy of the data analysis. Study concept and design: SJZ. Acquisition of data: JYZ, YTL, YYG, and CX. Analysis and interpretation of data: JYZ, YTL, YYG, and CX. Drafting of the article: SJZ. Statistical analysis: JYZ, XBZ, XWZ, and SJZ. Obtained funding: XBZ, XWZ, and SJZ. Study supervision: SJZ.

LITERATURE CITED

Ahissar E, Oram T. 2015. Thalamic relay or cortico-thalamic processing? Old question, new answers. Cereb Cortex 25:845–848.

Ahissar E, Zacksenhouse M. 2001. Temporal and spatial coding in the rat vibrissal system. Prog Brain Res 130:75–88.

Alitto HJ, Usrey WM. 2003. Corticothalamic feedback and sensory processing. Curr Opin Neurobiol 13:440–445.

Altman J, Bayer SA. 1979. Development of the diencephalon in the rat. IV. Quantitative study of the time of origin of neurons and the internuclear chronological gradients in the thalamus. J Comp Neurol 188:455–471.

Altman J, Bayer SA. 1988 Development of the rat thalamus: III. Time and site of origin and settling pattern of neurons of the reticular nucleus. J Comp Neurol. 275:406–428.

Altman J, Bayer SA. 1989. Development of the rat thalamus: V. The posterior lobule of the thalamic neuroepithelium and the time and site of origin and settling pattern of neurons of the medial geniculate body. J Comp Neurol 284:567–580.

Angevine JB. 1970. Time of neuron origin in the diencephalon of the mouse. An autoradiographic study. J Comp Neurol 139:129–188.

Bao XM, Shu SY. 1990. The stereotaxic atlas of the rat brain. Beijing, PR China: People's Health Publication Press.

Bass AH, Bodnar DA, Marchaterre MA. 2000. Midbrain acoustic circuitry in a vocalizing fish. J Comp Neurol 419:505–531.

Belekhova MG, Kenigfest-Rio NB, Vesselkin NP. 2002. Evolutionary significance of different neurochemical organization of the internal and external regions of auditory centers in the reptilian brain: an immunocytochemical and reduced NADPH-diaphorase histochemical study in turtles. Brain Res 925:100–106.

Brauth SE, Reiner A. 1991. Calcitonin-gene related peptide is an evolutionarily conserved marker within the aminote thalamo-telencephalic auditory pathway. J Comp Neurol 313:227–239.

Butler AB. 1994. The evolution of the dorsal thalamus of jawed vertebrates, including mammals: cladistic analysis and a new hypothesis. Brain Res Rev 19:29–65.

Cheng MF, Zuo MX. 1994. Proposed pathway for vocal self-stimulation: Met-enkephalinergic projections linking the midbrain vocal nucleus, auditory responsive thalamic regions and neurosecretory hypothalamus. J Neurobiol 5: 361–379.

Cornwall J. Cooper JD. Phillipson OT. 1990. Projections to the rostral reticular thalamic nucleus in the rat. Exp Brain Res 80:157–171.

Crespo C, Poteros A, Arévalo R, Briñón JG, Aijón J, Alonso RJ. 1999. Distribution of parvalbumin immunoreactivity in the brain of the *Tench Tinca tinca* L., 1758. J Comp Neurol 413:549–571.

Cuadrado MI. 1987. The cytoarchitecture of the torus semicircularis in the teleost *Barbus meridionalis*. J Morphol 191: 233–245.

Desbois C, Villanueva L. 2001. The organization of lateral ventromedial thalamic connections in the rat: a link for the distribution of nociceptive signals to widespread cortical regions. Neuroscience 102:885–898.

Dezso A, Schwarz DW, Schwarz IE. 1993. A survey of the auditory midbrain, thalamus and forebrain in the chicken (*Gallus domesticus*) with cytochrome oxidase histochemistry. J Otolaryngol 22:391–396.

Diamond ME. Armstrong-James M. Budway MJ. Ebner FF. 1992. Somatic sensory responses in the rostral sector of the posterior group POm and in the ventral posterior medial nucleus VPM of the rat thalamus: dependence on the barrel field cortex. J Comp Neurol 319:66–84.

Durand SE, Tepper JM, Cheng MF. 1992. The shell region of the nucleus ovoidalis: A subdivision of the avian auditory thalamus. J Comp Neurol 323:495–518.

Feng AS, Lin WY. 1991. Differential innervation patterns of three divisions of frog auditory midbrain (*torus semicircularis*). J Comp Neurol 306:613–630.

Franklin KB, Paxinos G. 1997. The mouse brain in stereotaxic coordinates. San Diego: Academic Press.

French CR, Sefton AJ, Mackay-Sim A. 1985. The inhibitory role of the visually responsive region of the thalamic reticular nucleus in the rat. Exp Brain Res 57:471–479.

Friedberg MH, Lee SM, Ebner FF. 1999. Modulation of receptive field properties of thalamic somatosensory neurons by the depth of anesthesia. J Neurophysiol 81:2243–2252.

Gould SJ. 1977. Ontogeny and phylogeny. Cambridge, MA: Belknap Press of Harvard University Press.

Groenewegen HJ, Berendse HW. 1994. The specificity of the 'nonspecific' midline and intralaminar thalamic nuclei. Trends Neurosci 17:52–57.

Guillery RW, Sherman SM. 2002. The thalamus as a monitor of motor outputs. Philos Trans R Soc Lond B Biol Sci 357:1809–1821.

Herbert P, Killackey, Murray S, Sherman. 2003. Corticothalamic projections from the rat primary somatosensory cortex. J Neurosci 23:7381–7384.

Herron P, Baskerville KA, Chang HT, Doetsch GS. 1997. Distribution of neurons immunoreactive for parvalbumin and calbindin in the somatosensory thalamus of the raccoon. J Comp Neurol 388:120–129.

Hevner RF, Liu S, Wong-Riley MT. 1995. A metabolic map of cytochrome oxidase in the rat brain: histochemical densitometric and biochemical studies. Neuroscience 65:313–342.

Huffman RF, Henson OW Jr. 1990. The descending auditory pathway and acousticomotor systems: connections with the inferior colliculus. Brain Res Rev 15:295–323.

Iwona S, Sharleen T, Sakai, Hui-xin Qi, Jon H. Kaas, 2003. Somatosensory Input to the ventrolateral thalamic region in the macaque monkey: a potential substrate for parkinsonian tremor. J Comp Neurol 455:378–395.

Jones EG. 1998. View point: the core and matrix of thalamic organization. J Neurosci 85:331–345.

Jones EG. 2001. The thalamic matrix and thalamocortical synchrony. Trends Neurosci 24:595–601.

Jones EG, Hendry SHC. 1989. Differential calcium binding protein immunoreactivity distinguishes classes of relay neurons in monkey thalamic nuclei. Eur J Neurosci 1:222–246.

Jones KR, Fariñas I, Backus C, Reichardt LF. 1994. Targeted disruption of the BDNF gene perturbs brain and sensory neuron development but not motor neuron development. Cell 76:989–999.

Khachunts AS, Belekhova MG. 1986. Characteristics of representations of the auditory and somatosensory systems in the thalamus of the turtle midbrain: electrophysiologic study. Neirofiziologiya 18:443–453.

Koralek KA, Jensen KF, Killackey HP. 1988. Evidence for two complementary patterns of thalamic input to the rat somatosensory cortex. Brain Res 463:346–351.

Lam YW, Sherman SM. 2010. Functional organization of the somatosensory cortical layer 6 feedback to the thalamus. Cereb Cortex 20:13–24.

Landisman CE, Connors BW. 2007. VPM and PoM nuclei of the rat somatosensory thalamus: intrinsic neuronal propertiesand corticothalamic feedback. Cereb Cortex 17: 2853–2865.

Lenz FA, Kwan HC,Martin RL, Tasker RR, Dostrovsky JO, Lenz YE. 1994. Single unit analysis of the human ventral thalamic nuclear group. Tremor-related activity in functionally identified cells. Brain 117:531–543.

Macchi G, Bentivoglio M. 1999. Is the "nonspecific" thalamus still "nonspecific?" Arch Ital Biol 137:201–226.

McAllister JP. Das GD. 1977. Neurogenesis in the epithalamus, dorsal thalamus and ventral thalamus of the rat: an autoradiographic and cytological study. J Comp Neurol 72:647–686.

McAlonan K, Brown VJ. 2002. The thalamic reticular nucleus: more than a sensory nucleus? Neuroscientist 8:302–305.

McCormick CA. 1999. Anatomy of the central auditory pathways of fish and amphibians. In: Fay RR, Popper AN, editors. Comparative hearing. New York: Springer. p 155–217.

McCormick CA. 2001. Brainstem acoustic areas in the marine catfish, Arius felis. Brain Behav Evol 57:134–149.

Miyata M. 2007. Distinct properties of corticothalamic and primary sensory synapses to thalamic neurons. Neurosci Res 59:377–382.

Monconduit L, Bourgeais L, Bernard JF, Le Bars D, Villanueva L. 1999. Ventromedial thalamic neurons convey nociceptive signals from the whole body surface to the dorsolateral neocortex. J Neurosci 19:9063–9072.

Monconduit L, Bourgeais L, Bernard JF, Villanueva L. 2003. Convergence of cutaneous muscular and visceral noxious inputs onto ventromedial thalamic neurons in the rat. Pain 103:83–91.

Münkle MC. Waldvogel HJ. Faull RLM. 2000. The distribution of calbindin, calretinin and parvalbumin immunoreactivity in the human thalamus. J Chem Neuroanat 19:55–173.

Muñoz A, Muñoz M, González A, Donkelaar H, Ten J. 1995. Anuran dorsal column nucleus: organization immunohistochemical characterization and fiber connections in *Rana perezi* and *Xenopus laevis*. J Comp Neurol 363: 197–220.

Northcutt RG. 1990. Ontogeny and phylogeny: a re-evaluation of conceptual relationships and some applications. Brain Behav Evol 36:116–140.

Northcutt RG. 2001. Evolution of the nervous system changing views of brain evolution. Brain Res Bull 55:663–674.

Orduz D, Boom A, Gall1 D, Brion JP, Schiffmann SN, Schwaller B. 2014. Subcellular structural plasticity caused by the absence of the fast $Ca2^{+}$ buffer calbindin D-28k in recurrent collaterals of cerebellar Purkinje neurons. Front Cell Neurosci 8:1–14.

Pare D, Smith Y, Parent A, Steriade M. 1988. Projections of brainstem core cholinergic and non-cholinergic neurone of cat to intralaminar and reticular thalamic nuclei. Neuroscience 25:69–86.

Paton JA, Kelley DB, Sejnowski TJ, Yodlowski ML. 1982. Mapping the auditory central nervous system of *Xenopus laevis* with 2-deoxyglucose autoradiography. Brain Res 249: 15–22.

Peruzzi D, Dut A. 2004. GABA, serotonin and serotonin receptors in the rat inferior colliculus. Brain Res 998:247–250.

Pritz MB, Stritzel ME. 1992. A second auditory area in the non-cortical telencephalon of a reptile. Brain Res 569: 146–151.

Puelles L, Robles C, Martinez-de-la-Torre M, Martinez S. 1994. New subdivision schema for the avian torus semicircularis: neurochemical maps in the chick. J Comp Neurol 340:98–125.

Puelles L, Kuwana E, Puelles E, Bulfone A, Shimamura K, Keleher J, Smiga S, John LR. 2000. Pallial and subpallial derivatives in the embryonic chick and mouse telencephalon, traced by the expression of the genes Dlx-2, Emx-1, Nkx-2.1, Pax-6, and Tbr-1. J Comp Neurol 424:409–438.

Rausell E, Jones EG. 1991. Histochemical and immunocytochemical compartments of the thalamic VPM nucleus in monkeys and their relationship to the representational map. J Neurosci 11:210–225.

Rausell E, Bae CS, Vinuela A, Huntley GW, Jones EG. 1992. Calbindin and parvalbumin cells in monkey VPL thalamic nucleus: distribution, laminar cortical projections, and relations to spinothalamic terminations. J Neurosci 12: 4088–4111.

Schellart NAM, Kamermans M, Nederstigt LJA. 1987. An electrophysiological study of the topographical organization of the multisensory torus semicircularis of the rainbow trout. Comp Biochem Physiol 88A:461–469.

Sherman SM. 2007. The thalamus is more than just a relay. Curr Opin Neurobiol 17:417–422.

Sherman SM. 2012. Thalamocortical interactions. Curr Opin Neurobiol 22:575–579.

Sherman SM, Guillery RW. 1996. Functional organization of thalamocortical relays. J Neurophysiol 76:1367–1395.

Sherman SM, Guillery RW. 1998. On the actions that one nerve cell can have on another: distinguishing "drivers" from "modulators." Proc Natl Acad Sci U S A 95:7121–7126.

Sherman SM, Guillery RW. 2002. The role of the thalamus in the flow of information to the cortex. Philos Trans R Soc Lond B Biol Sci 357:1695–1708.

Spreafico R, Barbaresi P, Weinberg RJ, Rustioni A. 1987. SII-projecting neurons in the rat thalamus: a single- and double-retrograde-tracing study. Somatosens Res 4:359–375.

Stepniewska I, Sakai ST, Qi H, Kaas JH. 2003. Somatosensory input to the ventrolateral thalamic region in the macaque monkey: a potential substrate for parkinsonian tremor. J Comp Neurol 455:378–395.

Striedter GF. 1997. The telencephalon of tetrapods in evolution. Brain Behav Evol 49:179–213.

Swanson LW. 1998. Brain maps: structure of the rat brain. Second revised edition. Amsterdam: Elsevier Science.

Veinante P, Jacquin MF, Deschenes M. 2000. Thalamic projections from the whisker-sensitive regions of the spinal trigeminal complex in the rat. J Comp Neurol 420:233–243.

Viaene AN, Petrof I, Sherman SM. 2011. Properties of the thalamic projection from the posterior medial nucleus to primary and secondary somatosensory cortices in the mouse. Proc Natl Acad Sci U S A 108:18156–18161.

Villanueva L, Bouhassira D, Bars DL. 1996. The medullary subnucleus reticularis dorsalis (SRD) as a key link in both the transmission and modulation of pain signals. Pain 67:231–240.

Villanueva L, Desbois C, Le Bars D, Bernard JF. 1998. Organization of diencephalic projections from the medullary subnucleus reticularis dorsalis and the adjacent cuneate nucleus: a retrograde and anterograde tracer study in the rat. J Comp Neurol 390:133–160.

Wild JM, Karten HJ, Frost BJ. 1993. Connections of the auditory forebrain in the pigeon Columba livia. J Comp Neurol 337:32–62.

Williams MN, Zahm DS, Jacquin MF. 1994. Differential foci and synaptic organization of the principal and spinal trigeminal projections to the thalamus in the rat. Eur J Neurosci 6:429–453.

Zeng SJ, Zhang XW, Peng WM, Zuo MX. 2004. Immunohistochemistry and neural connections of the Ov shell in a songbird, the Bengalese finch *Lonchura striata*. J Comp Neurol 470:192–209.

Zeng SJ, Jia Li, Xinwen Zhang, Mingxue Zuo. 2007a. Distinction of neurochemistry between the cores and their shells of auditory nuclei in tetrapod species. Brain Behav Evol 70:1–20.

Zeng SJ, Xi C, Zhang XW, Zuo MX. 2007b. Difference in neurogenesis between the core of auditory nuclei and their shelling areas in the turtle Pelodiscus sinensis and its evolutionary implications. Brain Behav Evol 70:174–186.

Zeng SJ, Tian CP, Zhang XW, Zuo MX. 2008a. Neurogenic development of the auditory areas of midbrain and diencephalon in the *Xenopus laevis* and evolutionary implications. Brain Res 1206:44–60.

Zeng SJ, Lin YT, Zhang XW, Zuo MX. 2008b. Comparative analysis of neurogenesis between the core and shell regions of auditory areas in the chick *Gallus gallus domesticus*. Brain Res 1216:24–37.

Zeng SJ, Lin YT, Tian CP, Zhang XW, Zuo MX. 2009. Evolutionary significance of delayed neurogenesis in the core versus shell auditory areas of *Mus musculus*. J Comp Neurol 515:600–613.

Xi C, Zeng SJ, Lin YT, Huang YF, Liu Y, Zhang XW, Zuo MX. 2011. Sites of origin and migrating routes of the neurons in the core and shell regions of torus semicircularis in the chinese soft shell turtle (*Pelodiscus sinensis*). J Comp Neurol 519:2677–2696.

Yang ZG, You Y, Levison SW. 2008. Neonatal hypoxic/ischemic brain injury induces production of calretinin-expressing interneurons in the striatum. J Comp Neurol 511:19–33.

Yu C, Horev G, Rubin N, Derdikman D, Haidarliu S, Ahissar E. 2015. Coding of object location in the vibrissal thalamocortical system. Cereb Cortex 25:563–577.